

Potential Reproducibility of Potassium-Selective Electrodes Having Perfluorinated Alkanoate Side Chain Functionalized Poly(3,4-ethylenedioxythiophene) as a Hydrophobic Solid Contact

Soma Papp,[†] Márton Bojtár,[‡] Róbert E. Gyurcsányi,[†] and Tom Lindfors^{*,§}

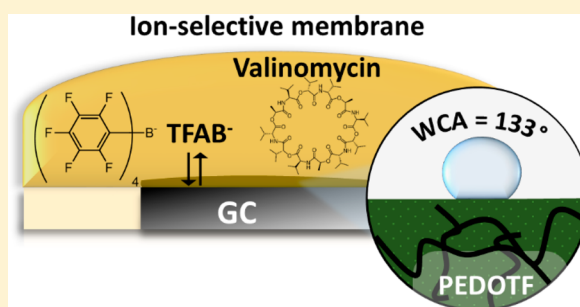
[†]Department of Inorganic and Analytical Chemistry, Chemical Nanosensor Research Group, Budapest University of Technology and Economics, Szt. Gellért tér 4, H-1111 Budapest, Hungary

[‡]Chemical Biology Research Group, Institute of Organic Chemistry, Research Centre for Natural Sciences, Hungarian Academy of Sciences, Magyar tudósok krt. 2, H-1117 Budapest, Hungary

[§]Åbo Akademi University, Faculty of Science and Engineering, Laboratory of Analytical Chemistry, Biskopsgatan 8, FIN-20500 Åbo, Finland

Supporting Information

ABSTRACT: The irreproducibility of the standard potential (E°) is probably the last major challenge for the commercialization of solid-contact ion-selective electrodes (SCISEs) as single-use or wearable sensors. To overcome this issue, we are introducing for the first time a perfluorinated alkanoate side chain functionalized poly(3,4-ethylenedioxythiophene) (PEDOTF) as a hydrophobic SC in potassium-selective electrodes (K-SCISEs) based on plasticized poly(vinyl chloride). The SC incorporates the tetrakis-(pentafluorophenyl)borate (TFAB⁻) anion, which is also present as a lipophilic additive in the ion-selective membrane (ISM), thus ensuring thermodynamic reversibility at the SC/ISM interface and improving the potential reproducibility of the electrodes. We show here that the PEDOTF-TFAB solid contact, which was prepolarized prior to the ISM deposition to either its half or fully conducting form (i.e. different oxidation states) in acetonitrile containing 0.01 M KTFAB, had a very stable open-circuit potential and an outstanding potential reproducibility of only ± 0.5 mV ($n = 6$) for 1 h in the same solution after the prepolarization. This shows that the oxidation state of the highly hydrophobic PEDOTF-TFAB film (water contact angle 133°) is stable over time and can be precisely controlled with prepolarization. The SC was also not light sensitive, which is normally a disadvantage of conducting polymer SCs. After the ISM deposition, the standard deviation of the E° of the K-SCISEs prepared on glassy carbon was ± 3.0 mV ($n = 5$), which is the same as that for conventional liquid contact K-ISEs. This indicates that the ISM deposition is the main source for the potential irreproducibility of the K-SCISEs, which has been overlooked previously.



organic frameworks (MOF),²⁹ and different types of composite materials.^{30–37}

Initially the main aim of the research in this field was to develop robust and miniaturized SCISEs that match the excellent potential stability of the conventional ISEs with a potential drift of less than ca. 0.1 mV h^{-1} . However, with the increasing interest in single-use and wearable sensors,^{38,39} the efforts became largely oriented toward the development of SCISEs for calibration-free measurements. ISEs seem ideal devices in this respect, as they follow the Nernst equation: i.e., the slope of the linear part of the calibration curve (E vs $\log a_i$) is constant for a given analyte ion charge and temperature. Properly designed SCISEs have slopes very close to the ideal Nernstian slope, but their standard potentials (E°) determined

Solid-contact ion-selective electrodes (SCISEs) have been the subject of intensive research. Clearly, the replacement of the aqueous liquid contact in conventional ISEs with a solid material is appealing not only in terms of widening their applicability by withstanding higher pressures (deep water measurements) or temperatures but also in terms of easier mass production and robust miniaturization.¹ The most popular ion-to-electron transducers, i.e. solid contacts (SC), have been until now electrically conducting polymers (ECP),^{2–10} different carbon materials with large capacitance,^{11–15} redox couples,^{16,17} and redox-active compounds.¹⁸ Recently various new SCs have also grown in popularity, such as tetrathiafulvalene (TTF)¹⁹ and 7,7,8,8-tetracyanoquinodimethane (TCNQ) and their radical salts,²⁰ intercalation compounds (LiFePO₄/FePO₄),²¹ Prussian blue analogues,²² KBr/AgBr,²³ fullerenes,²⁴ submicron porous carbon spheres,²⁵ gold nanoparticles,^{26,27} molybdenum disulfide,²⁸ metal–

Received: March 29, 2019

Accepted: June 11, 2019

Published: June 11, 2019

at $a_i = 0$ usually show an unacceptable large variation. Not only are the E° values difficult to predict theoretically but also even the very same preparation method may lead to unreproducible values, which is currently the biggest challenge hampering commercialization of the SCISEs.

Although some very good E° reproducibilities have been reported, it is still problematic to objectively compare these values due to the lack of a standardized test protocol for the E° determination. The SCISEs may have been exposed to conditioning or measurements for different long periods before the standard deviation (SD) of E° was determined. While a divergence in time of the E° values is the most common, there are also examples of the opposite. For example, K^+ -selective SCISEs (K-SCISEs) with the SC composed of polyaniline dispersed in a plasticized poly(vinyl chloride) ion-selective membrane (PVC-ISM) had an initial E° reproducibility of ± 17.9 mV ($n = 3$) after 1 day but improved to only ± 1.9 mV after 57 days of exposure to 0.1 M KCl.⁶ Until now, the highest E° reproducibility of ± 0.1 mV ($n = 5$) has been obtained by Paczosa-Bator for K-SCISEs, which were prepared with a relatively complex SC consisting of highly porous graphene, carbon black, and a fluorinated acrylic copolymer. The SC lacks a redox couple and therefore a well-defined interfacial charge transfer mechanism.³³ A slightly lower E° reproducibility of ± 0.3 mV ($n = 5$) was reported for a nitrate-selective SCISE prepared with the TTF/TTF⁺ redox couple and graphene as the nanocomposite SC.³¹

Redox couples/materials soon emerged as the most promising approaches to theoretically adjust the E° value of the SCISEs by the simplicity of varying the ratio of the redox components. Indeed, the pioneering work of Zou et al. incorporating a redox couple consisting of the Co(II) and Co(III) complexes of 1,10-phenanthroline in the PVC-ISM proved to be beneficial in obtaining a high initial E° reproducibility of ± 0.7 mV ($n = 5$) for K-SCISEs.¹⁷ However, the reproducibility deteriorated to ± 16.3 mV already after 24 h due to leaching of the redox compound(s) to the aqueous phase, showing that this concept still needs to be technically improved. Using a similar approach that was introduced by Jaworska et al.,³⁵ a E° reproducibility of only ± 0.2 mV ($n = 3$) was achieved by incorporating two organometallic complexes of Co(II) and Co(III) (not a redox couple) into the ISM.¹⁸ In another innovative concept by Ishige et al., the LiFePO₄/FePO₄ redox couple (intercalation compounds) was used as the SC in Li⁺-selective SCISEs, resulting in a good E° reproducibility of ± 2.0 mV ($n = 3$).²¹

Electrically conducting polymers usually have a rather broad distribution of redox states, and therefore the E° (SD) of the ECP-based SCISEs is usually ca. ± 10 – 20 mV or even higher.⁴⁰ However, their E° reproducibility can be efficiently improved by prepolarization of the ECP-SC before the deposition of the PVC-ISM on top of it,^{8,9,41,42} by short-circuiting the SCISEs to a reference electrode (RE),⁴⁰ or by applying a potential or a current pulse in the nA range to the electrodes.⁴³ The prepolarization is undeniably the simplest and quickest method of adjusting the conducting state of the ECPs, which we found essential in obtaining a good E° reproducibility for K-SCISEs in our previous studies.^{8,9} It is crucial that the ECP is prepolarized to its half or fully conducting form to ensure thermodynamic reversibility at the SC/ISM interface. In addition, it is equally important that the ECP is hydrophobic enough to prevent the formation of the detrimental aqueous layer at the SC/ISM interface that results in response

instability. This is normally not the case, because the ECP backbone is positively charged in its conducting form, making it relatively hydrophilic.

To overcome this limitation, we have shown recently that the incorporation of a highly hydrophobic anion such as perfluorooctanesulfonate (PFOS) in the polypyrrole (PPy) matrix makes the ECP very hydrophobic in its conducting form (water contact angle (WCA): $97 \pm 5^\circ$). K-SCISEs based on such prepolarized SCs had a very good E° reproducibility of ± 0.7 mV ($n = 4$) and a very low potential drift of only $69 \mu\text{V h}^{-1}$ during the test period of 46 days, after which they still had a good E° reproducibility of ± 3.1 mV. Other studies,^{31,33} including that of Guzinski et al. using PEDOT-C₁₄ as the SC,¹⁰ seem to conclusively support the need for highly hydrophobic SCs as one of the main prerequisites for obtaining stable and reproducible electrode potentials. Despite the good E° reproducibility of the K-SCISEs based on PPy-PFOS, we observed in interlaboratory studies that it was challenging to get a very good E° reproducibility with a larger number of SCISEs.

We have therefore conducted a systematic study to understand the reasons for the E° irreproducibility of K-SCISEs having poly(3,4-ethylenedioxythiophene) (PEDOT) as the SC. For the first time a highly hydrophobic perfluorinated alkanolate side chain functionalized PEDOT^{44,45} (PEDOTF) has been applied as the SC. It incorporates the tetrakis(pentafluorophenyl)borate anion (TFAB⁻) in its structure to enhance the hydrophobicity of the conducting form of the ECP-SC. To further optimize the SCISE design, we have also added TFAB⁻ to the ISM as a lipophilic cation exchanger, which we expect will result in a well-defined and reproducible phase boundary potential at the SC/ISM interface. The results presented in this work show that the deposition of the PVC-ISM on the SC is the main source causing the potential irreproducibility of the K-SCISEs, which has been overlooked previously.

EXPERIMENTAL SECTION

Chemicals. As described in the Supporting Information, fluorinated 3,4-ethylenedioxythiophene with a perfluorooctanyl side chain (EDOTF) was custom-synthesized from hydroxymethyl EDOT (95%) and pentadecafluorooctanoyl chloride (97%) obtained from Sigma-Aldrich. High-molecular-weight PVC (HMW PVC), bis(2-ethylhexyl) sebacate (DOS), potassium ionophore I (valinomycin), and tetrahydrofuran (THF), all Selectophore grade, and anhydrous acetonitrile (ACN; 99.5%) were purchased from Sigma-Aldrich. KTFAB (97%; Figure S-1) was obtained from Alfa Aesar, and KCl (99.999%, Suprapur grade) was received from Merck Millipore. All aqueous solutions were prepared from deionized water (DIW) with a resistivity of 18.2 M Ω cm (ELGA).

Electropolymerization of EDOTF and Prepolarization of the PEDOTF-SCs. The electropolymerization (EP) of EDOTF was done galvanostatically at 0.5 mA cm⁻² to 0.5 C cm⁻² (controlled by a Autolab PGSTAT potentiostat) in freshly made ACN solutions of 0.01 M EDOTF and 0.01 M KTFAB. A three-electrode setup was used, where a glassy-carbon (GC) or gold electrode ($d = 1.6$ mm; incorporated in a polyether ether ketone (PEEK) body with an outer diameter of 6.0 mm; Bio-Logic Science Instruments), a Pt wire, and a Ag wire served as working (WE), counter, and pseudo-RE, respectively. The WE was polished prior to the EP with a 0.05 μm alumina suspension, rinsed thoroughly with ethanol

and DIW followed by ultrasonication for 5 min in DIW, and finally rinsed again with ethanol and DIW. The electropolymerization solution was first purged with N_2 for 15 min immediately before use and then blanketed during the polymerization. After the EP, the PEDOTF-TFAB films were rinsed with ACN and prepolarized in deaerated 0.01 M KTFAB-ACN at either 0.22 or 0.40 V for 5 min using the same three-electrode setup as above. Finally, the PEDOTF-SCs were rinsed with either ACN or THF, as explained in the [Results and Discussion](#), before they were allowed to dry for ca. 10 min in ambient air prior to the drop-casting of the PVC-ISM on top of the PEDOTF-SC. Some of the PEDOT-TFAB films were also characterized after the EP with cyclic voltammetry (CV) in the potential range of -0.5 V to $+0.7$ V in deaerated 0.01 M KTFAB-ACN with scan rates (ν) of 5, 10, and 20 $mV s^{-1}$ using the same three-electrode setup as above. All electrode potentials in this work related to the electropolymerization of EDOTF, prepolarization, and characterizations of the PEDOTF-SCs refer to the Ag wire acting as a pseudoreference electrode.

K⁺-Selective SCISE Fabrication. The ISM had the following composition: 32.9% (w/w) HMW PVC, 65.7% DOS, 1.06% valinomycin, and 0.34% KTFAB. The components were dissolved in 1 mL of THF to produce a solution with 20% dry weight. A 40 μL portion of the ISM cocktail solution was deposited by drop-casting onto the PEDOTF-SCs in two consecutive steps ($2 \times 20 \mu L$), and the PVC-ISM with a thickness of ca. 220 μm were allowed to dry overnight in ambient air. We compared the initial potential stability and E° reproducibility of the K-SCISE with those of their conventional liquid contact counterparts having the same ISM composition. The latter were prepared by pouring 1.5 mL of an ISM cocktail (10% w/w in THF) into a glass ring ($d = 24.4$ mm) fixed on a glass plate. The PVC-ISM was allowed to dry overnight before circular membranes with a diameter of 7 mm were punched (thickness ca. 200 μm) out of it and mounted into conventional Philips IS 561 electrode bodies (Möller Glasbläserei, Zürich, Switzerland) with 0.01 M KCl as the inner filling solution.

Potentiometric Measurements. We used a 16-channel high input impedance voltmeter ($10^{15} \Omega$, Lawson Laboratories, Malvern, PA, USA) in all potentiometric measurements. The potential stability of the PEDOTF-SCs was determined in 0.01 M KTFAB-ACN for 1 h, whereas the initial potential stabilities of the K-SCISEs were measured in 0.01 M KCl for 24 h. The K-SCISEs were calibrated from 10^{-1} to 10^{-9} M KCl, and the potential readings at every concentration were taken after 5 min in quiescent solutions. In all aqueous solutions, we used a double-junction Ag/AgCl/3 M KCl//1 M LiOAc as the RE (No. 6.0729.100, Metrohm AG). The potentiometric aqueous layer test was done with fully conditioned SCISEs by changing the solution from 0.1 M KCl to 0.1 M NaCl (24 h) and then back to 0.1 M KCl (24 h). The light sensitivity of the PEDOTF-SC (without ISM) was measured in 0.01 M KTFAB-ACN by keeping the electrodes first in room light (10 min) and then exposing them to complete darkness (10 min) and finally to intense cold light (10 min, $>1.6 \times 10^5$ lx; Leica CLS 150XE light source⁴¹).

Water Contact Angles and SEM Measurements. Water droplets were placed on PEDOTF-TFAB films ($d = 5.0$ mm) that had been prepolarized to -0.50 , 0.20 , and 0.50 V. We recorded images of the water droplets with a Dyno-Lite USB digital microscope and determined the WCAs from the images

with the Inkscape 0.92.3 software. We measured the surface morphology and the film thickness of the PEDOTF-SC prepared on a Pt-sputtered ZnSe reflection element (see below) with the LEO1530 Gemini FEGSEM instrument.

Water Uptake of the PEDOTF-SC. We measured the diffusion of water in the ca. 1.8 μm thick PEDOTF-SC with the FTIR-ATR technique for 24 h in 0.01 M KCl. The film was deposited by electropolymerization on the Pt-sputtered ZnSe reflection element. Prior to the water uptake measurements, we prepolarized the SC to its fully conducting form (positively charged) at 0.40 V for 5 min to maximize its water uptake. The experimental details of the water uptake measurements are given in the [Supporting Information](#). The experimental setup and the modeling of the water diffusion coefficients have been thoroughly described in detail elsewhere.^{9,46}

RESULTS AND DISCUSSION

We report here for the first time the electropolymerization of EDOTF with the TFAB⁻ anion as the charge-compensating counterion on GC and gold (Au) substrates. [Figure S-2](#) shows the CVs recorded during the electropolymerization of 0.01 M EDOTF in 0.01 M KTFAB-ACN on GC in the potential range of -0.9 to $+1.5$ V. They reveal that the polymerization of EDOTF starts at ca. 1.3 V, and the increasing anodic and cathodic currents confirm that the film grows in thickness during each potential cycle. However, we found that the PEDOTF film growth was not fully reproducible with CV and the PEDOTF-SC film thickness could not therefore be controlled precisely. Some GC electrodes required a higher anodic end potential for the film formation, which may be due to slightly different surface properties of the commercial GC-PEEK electrodes used in this study. This assumption is supported by comparing the anodic and cathodic peak potentials (E_{pa} , E_{pc}) given by the electrode manufacturer for the 12 GC-PEEK electrodes that were used in this study. The manufacturer had measured the E_{pa} and E_{pc} after the electrode fabrication in 1 mM $K_4Fe(CN)_6$ with 1.0 M KNO_3 as the background electrolyte. The comparison shows that the E_{pa} varied between 237 and 295 mV for the 12 GC-PEEK electrodes that were supposed to be identical (electrodes 1–9, 289 ± 4 mV; electrodes 10–12, 238 ± 1 mV). The corresponding E_{pc} values were 162–225 mV (electrodes 1–9, 220 ± 6 mV; electrodes 10–12, 163 ± 1 mV), and the peak separation ($\Delta E_p = E_{pa} - E_{pc}$) was 64–75 mV. It is known that the electron transfer for GC is affected by surface functional groups (carbonyl, carboxyl, and hydroxyl), and their surface concentration can be influenced if the electrodes are polished in the presence of water.⁴⁷ Moreover, adsorption of organic contaminants from ultrapure water and ambient air has been identified to lower the electroactivity of a highly oriented pyrolytic graphite surface, which can also affect the electroactivity of GC.⁴⁸

We decided therefore to perform the electropolymerization galvanostatically with a constant current of 0.5 mA cm^{-2} , which allowed us to better control the charge consumed during the electropolymerization (0.5 C cm^{-2}) and ensure that all PEDOTF-SCs had the same thickness (i.e. redox capacitance). To minimize the variation of the initial surface state of the individual electrodes, we polished them repeatedly until they had $\Delta E_p = 75$ mV when the GC-PEEK electrodes were characterized by CV in 2 mM $K_4Fe(CN)_6$ with 1.0 M KNO_3 as the background electrolyte ($\nu = 5$ mV s^{-1} ; [Figure S-3](#)). After the CV characterization, the E_{pa} and E_{pc} values of the

electrodes were typically 292–294 and 215–217 mV, respectively. To further improve the reproducibility of the electropolymerization, the PEDOTF-TFAB electrodes were individually electropolymerized from fresh monomer solutions ($V = 3$ mL, Figure S-4). The formed PEDOTF-SCs were characterized by CV in 0.01 M KTFAB-ACN in the potential range of -0.5 to $+0.5$ V (Figure 1). The CVs show that the

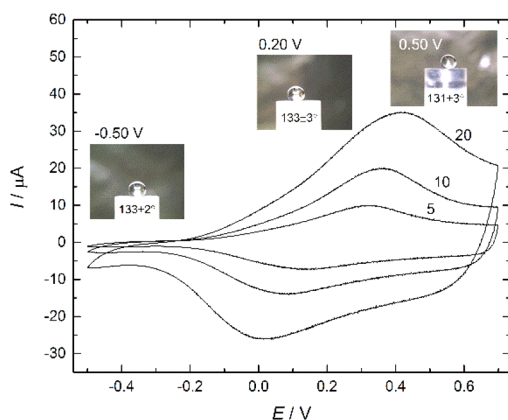


Figure 1. CVs of the PEDOTF-SC in 0.01 M KTFAB-ACN measured with the scan rates of 5, 10, and 20 mV s^{-1} . The insets show the WCAs of the PEDOTF-SC that was polarized to -0.50 , 0.20 , and 0.50 V in same electrolyte solution (vs a Ag wire).

PEDOTF film converts to the electrically conducting form at $E > -0.20$ V. At $\nu = 5$ mV s^{-1} , the E_{pa} and E_{pc} values were 0.32 and 0.13 V, respectively, but shifted to 0.42 and 0.02 V for $\nu = 20$ mV s^{-1} , indicating that the electrode transfer becomes slightly more sluggish at higher scan rates.

SEM images (Figure S-5) revealed that the PEDOT-TFAB film has a uniform surface morphology and a relatively open surface structure with sharper polymer bundles pointing out from the surface, which are expected to further lower the wettability of the hydrophobic polymer film. To confirm this, we performed WCA measurements on PEDOTF-SCs prepolarized to -0.5 V (nonconducting form), 0.20 V (half conducting form), and 0.5 V (fully conducting form) in 0.01 M KTFAB-ACN. In agreement with our expectations, the WCA of PEDOTF was ca. 131 – 133° irrespective of its conducting state (insets in Figure 1), proving that both the half and fully conducting forms are highly hydrophobic, which is crucial for preventing the detrimental aqueous layer formation beneath the ISM causing potential instability of the SCISEs. The WCAs reported here are slightly lower than those measured by Luo et al. for a PEDOTF film prepared with a constant potential of 1.4 V at 0°C (131.9 – 150.5°)⁴⁵ but are in very good accordance with the WCA of PEDOT- C_{14} ($136 \pm 5^\circ$) and higher than those for polyazulene doped with PF_6^- (PAZ- PF_6 ; $126 \pm 14^\circ$),⁴² chemically prepared polyoctylthiophene (POT; ca. 110°),⁴⁹ and PPy-PFOS ($97 \pm 5^\circ$).¹⁰

The high hydrophobicity of the PEDOTF-SC film was confirmed by measuring the water diffusion through the film with the FTIR-ATR technique^{46,50–52} when it was placed in contact with 0.01 M KCl solution (Figure 2). In evaluating the FTIR spectra, it must be kept in mind that this technique is very sensitive and is able to detect traces of water, in contrast to the potentiometric aqueous layer test.⁵³ The spectra in the wavenumber region of ca. 3000 – 3700 cm^{-1} (OH stretching) reveal that minor amounts of water have diffused through the

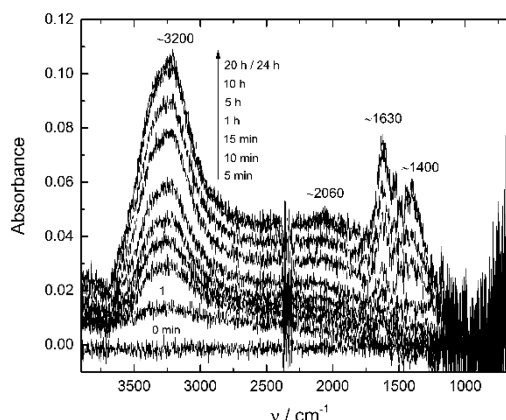


Figure 2. Water uptake of the bare PEDOTF-SC measured after 0, 1, 5, 10, and 15 min and 1, 5, 10, 20, and 24 h in contact with 0.01 M KCl. The SC was polarized in 0.01 M KTFAB-ACN at 0.40 V (vs a Ag wire) prior to the water uptake measurement. Gain factor: 128.

PEDOTF-SC to the vicinity of the SC/ZnSe interface already after 5 min when the SC is fully exposed to water. The amount of water increases very slowly during the whole measurement until a saturation level is reached after ca. 20 h. It is expected that some water diffusion will always take place in all types of (slightly) porous SCs, showing the challenge in completely blocking the water diffusion. Mathematical modeling of the water uptake showed that it can be described with three diffusion coefficients, $D_1 = 6.6 \times 10^{-11}$ $\text{cm}^2 \text{s}^{-1}$, $D_2 = 1.9 \times 10^{-12}$ $\text{cm}^2 \text{s}^{-1}$, and $D_3 = 2.8 \times 10^{-13}$ $\text{cm}^2 \text{s}^{-1}$, indicating that the water diffusion in the PEDOTF-SC is slightly higher than in the PPy-PFOS solid contact⁹ but lower than in the POT-SC.⁵¹ However, as the surface of most conducting polymers is relatively uneven, it is difficult to determine the film thickness with the highest precision, adding some uncertainty to the reported water diffusion coefficients.

The SC should preferably have a relatively high capacitance to provide the SCISEs with a stable potential.⁴ Electrochemical impedance measurements showed that the redox capacitance of the PEDOTF-SC was ca. 40 mF cm^{-2} (Figure S-6). This is sufficiently high for the PEDOTF-SC to act as very efficient redox buffer and ion-to-electron transducer in the K-SCISEs. The capacitance is considerably higher than for PEDOT prepared with polystyrenesulfonate (15 mF cm^{-2}),⁵⁴ similar to that for PAZ- PF_6 (45 mF cm^{-2}),⁴² and much lower than that for a composite consisting of polyaniline and reduced graphene oxide (77 mF cm^{-2}).⁵⁵ All transducers were prepared with the same charge as for the PEDOTF-SC.

The lipophilic TFAB⁻ anion is present both in the PVC-ISM and in the PEDOTF-SC to ensure thermodynamic reversibility at the SC/ISM interface. We measured therefore the potentiometric response of the SC in 10^{-4} – 10^{-2} M KTFAB-ACN and in aqueous 10^{-4} – 10^{-1} M KCl solutions to determine if the PEDOTF-SC exchange anions or cations. We found that the SC had a super-Nernstian anionic response in KTFAB-ACN solutions, revealing that it is exchanging TFAB⁻ anions when the SC is in contact with an organic phase: i.e., the PVC-ISM. In KCl solutions, we observed a sub-Nernstian K^+ response indicating that the highly hydrophobic TFAB⁻ anion cannot leave the SC and enter the aqueous phase. We can therefore conclude that the PEDOT-SC exchanges TFAB⁻ anions when it functions as an ion-to-electron transducer beneath the K^+ -selective PVC-ISM, which

we expect will improve the potential reproducibility of the electrodes. However, we can speculate that a certain degree of K^+ exchange may also occur in the presence of small amounts of water at the SC/ISM interface.

The light sensitivity can be a drawback for most ECPs, especially POT,⁴¹ although many ECPs that we have used as SCs in SCISEs, such as PPy-PFOS⁹ and PAz-PF₆,⁸ are completely light insensitive beneath the ISM. We therefore measured the potential response of only the bare PEDOTF-SC in 0.01 M KTFAB-ACN (to exclude the influence of the ISM) when the SC was exposed to room light, complete darkness, and intense cold light (Figure 3). We did not observe any light

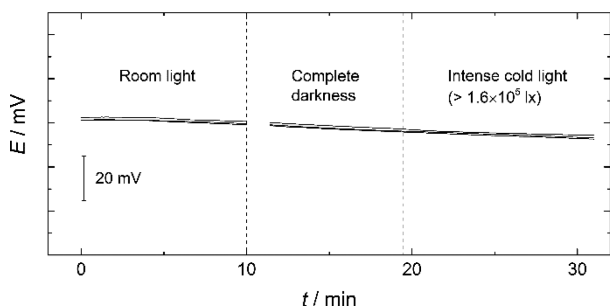


Figure 3. Light sensitivity of the PEDOTF-SCs ($n = 3$) measured in 0.01 M KTFAB-ACN by exposing it to room light, darkness, and intense cold light ($>1.6 \times 10^5$ lx). The SC was prepolarized to 0.40 V (vs a Ag wire) in the same electrolyte solution before starting the measurement. The minor potential drift is due to the evaporation of ACN from the solution.

sensitivity of the bare PEDOTF-SC, thus making it a most suitable SC material for SCISEs. The light sensitivity test was restricted to 30 min due to the high volatility of ACN, which is the reason for the slow potential drift observed in Figure 3.

To identify what causes the E° irreproducibility of the K-SCISEs, we started by measuring the potential stability of the bare PEDOTF-SC before the ISM was deposited on top of it by drop-casting. The PEDOTF-SC was first prepolarized to 0.22 V for 5 min in 0.01 M KTFAB-ACN, and after that, its open-circuit potential stability and reproducibility were measured in the same electrolyte solution for 1 h (Figure 4).

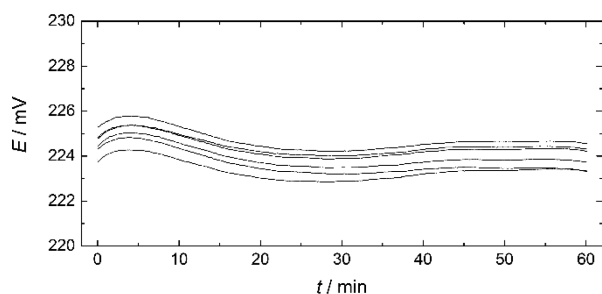


Figure 4. Potential stability and reproducibility of the PEDOTF-SC ($n = 6$) measured in 0.01 M KTFAB-ACN for 1 h after polarization in the same solution to 0.22 V (vs a Ag wire) for 5 min.

The PEDOTF-SCs showed an outstanding potential stability and a potential reproducibility (given as the SD) of ± 0.5 mV ($n = 6$) during the whole test period. This shows that it is possible to adjust the conducting state of the PEDOTF-SC to a desired level that is very stable over time. The measurement proved also that differences in the initial surface conditions of

the GC substrates do not influence the potential reproducibility of the prepolarized SCs, and we can therefore exclude that they cause the E° irreproducibility of the SCISEs.

Since the PEDOTF-SC will be in contact with THF during the drop-casting of the PVC-ISM on top of it, we studied also how the potential reproducibility was influenced by keeping the SC in contact with a pure stirred THF solution for different long times up to 30 min. After the SC was kept in pure THF solution for 0.25, 0.5, 1, 2, 5, 10, 15, or 30 min, its potential reproducibility was determined at the open-circuit potential in 0.01 M KTFAB-ACN (Figure 5).

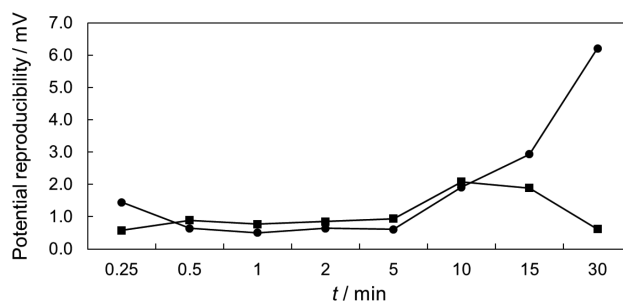


Figure 5. Potential reproducibility (given as SD) of the PEDOTF-SC ($n = 6$) measured in 0.01 M KTFAB-ACN after different exposure times to stirred (■) THF and (●) ACN. We ensured that the SC had the same initial oxidation state (i.e. conducting form) in all measurements by polarizing it to 0.22 V (vs a Ag wire) in 0.01 M KTFAB-ACN for 5 min before each measurement.

We compared the potential reproducibilities obtained after the THF treatment with a PEDOTF-SC that had been exposed to pure ACN in an identical measuring sequence. This was done because the SC is rinsed with pure ACN after the prepolarization in 0.01 M KTFAB-ACN and it can possibly influence its doping level (i.e. oxidation state) due to leaching of TFAB⁻ anions into the organic solvent. Figure 5 shows that the contact time with THF does not influence the potential reproducibility to any significant extent, especially for $t \leq 5$ min (SD < 1.0 mV). Even for greater exposure times there is no clearly observed trend, and since the potential reproducibility is still ± 0.6 mV after the contact time of 30 min with THF, which is the same as for $t = 0.25$ min, it is unlikely that THF will affect the potential of the PEDOTF-SC during the drop-casting and overnight drying of the PVC-ISM. However, we found that a contact time longer than 5 min with ACN had a negative effect on the potential reproducibility. Hence, the PEDOTF-SC should be rinsed only briefly to remove residues of the KTFAB electrolyte salt from its surface. In another experiment described in Figure S-7, we show that it is essential to rinse the SC with ACN after the prepolarization to avoid severe deterioration of the detection limit (LOD) and selectivity coefficients of the K-SCISEs.

We fabricated the K-SCISEs on GC and Au substrates to study how the substrate material influences the initial potential stability and reproducibility of the electrodes (Figure 6 and Figure S-8). The PEDOTF-SCs were prepolarized either to the half-conducting form (0.22 V) or fully conducting form (0.40 V) in 0.01 M KTFAB-ACN. They were then kept in a stirred ACN solution for 30 s to wash off KTFAB residues from the SC surface. We let the SCs dry in ambient air for ca. 10 min prior to the deposition of the PVC-ISM by drop-casting.

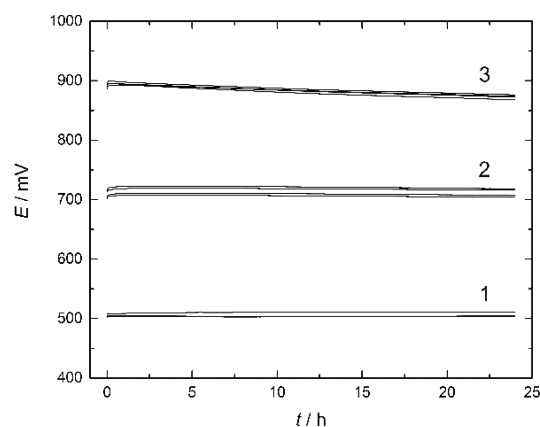


Figure 6. Initial potential stability and reproducibility of (1) conventional liquid contact K-ISEs ($n = 5$) and K-SCISEs prepared with the PEDOTF-SC prepolarized to (2) 0.22 V ($n = 4$) and (3) 0.40 V ($n = 5$) in 0.01 M KTFAB-ACN (vs a Ag wire). The SCISEs were fabricated on GC, and the measurements were carried out for 24 h in 0.01 M KCl. The potentials of the conventional ISEs have been shifted with 370 mV to higher potentials.

When the SCISEs were in contact with 0.01 M KCl solution for the first time, the potential of the K-SCISEs prepared on GC substrates stabilized quickly within ca. 3–5 min independent of the prepolarization potential of the PEDOTF-SC (Figure 6), which is only slightly longer than that for the conventional liquid contact K-ISEs (ca. 2 min). We obtained the same stabilization time of 3–5 min for the SCISEs prepared on Au substrates with the PEDOTF-SC prepolarized to 0.22 V, while the electrodes prepolarized to 0.40 V had a considerably longer stabilization time of ca. 20 min (Figure S-8).

In Table 1, we have summarized the potential drifts and potential reproducibilities (SD) of the K-SCISEs and conventional liquid contact K-ISEs measured during the initial potential stability measurement. The SCISEs prepared on the GC substrates had a slightly better potential reproducibility, especially after 24 h in contact with 0.01 M KCl, than the SCISEs having Au as the substrate material. Among all electrodes, the K-SCISEs prepared on GC and prepolarized at 0.40 V had the best potential reproducibility of only ± 3.3 mV at the beginning of the test ($t = 0$ h) and ± 2.7 mV after 24 h. This is practically the same as for the conventional K-ISEs, which showed ± 2.1 and ± 2.9 mV at the beginning of the test and after 24 h,

respectively. This indicates that the prepolarized K-SCISEs have response characteristics that are equal to those of the conventional K-ISEs. It also shows that the prepolarization of the SC is essential to obtain electrodes with high E° reproducibility. We demonstrate this in Figure S-9 for K-SCISEs having nonpolarized PEDOTF-SCs. The potential response of one of the SCISEs deviates considerably (>300 mV) from the other five electrodes, which show a relatively good E° reproducibility of ± 5.2 mV in the beginning of the initial potential stability test (Table 1), but ± 10.7 mV already after 24 h in 0.01 M KCl.

We observed that the K-SCISEs that were prepolarized to the half conducting form (0.22 V) had a lower initial potential drift in comparison to the electrodes prepolarized to the fully conducting form (0.40 V). The K-SCISEs fabricated on GC and prepolarized to 0.22 V had the lowest potential drift of only $-56 \pm 24 \mu\text{V h}^{-1}$ during the first 24 h in 0.01 M KCl, which is comparable to the drift of the conventional K-ISEs ($32 \pm 47 \mu\text{V h}^{-1}$). The reasons for the higher drift obtained for the K-SCISEs prepolarized at 0.40 V is still unclear. However, we speculate that the long-term stability of the fully oxidized form of PEDOTF-SC is lower than that for the half oxidized form (0.22 V), which has approximately equal concentrations of conducting and nonconducting polymer segments, thus providing the SCs with a better redox buffer capacity: e.g., against the influence of oxygen. Figure S-10 shows that the potential of the K-SCISE prepared on GC and prepolarized at 0.22 V was insensitive to O_2 and CO_2 when these gases were purged through 0.1 M KCl for 95 and 60 min, respectively. We note also that we did not study further the potential response characteristics of the K-SCISEs fabricated on the Au substrates due to their slightly worse potential reproducibility in comparison to GC.

Completely new Au and GC electrodes were also bought for this purpose and were compared to older GC electrodes that were purchased in 2010, which had been in extensive use earlier. We could not find any noticeable differences in the initial potential stability and reproducibility between these GC electrodes and the new GC electrodes that were purchased for this project.

In Figure 7, the calibration curves show that the K-SCISEs prepared on GC with the PEDOTF-SC prepolarized to the fully conducting form had in practice the same potentiometric response as the conventional K-ISEs. The E° reproducibility (SD), slope, and LOD of the K-SCISEs and the conventional

Table 1. Initial Potential Drift and Reproducibility in 0.01 M KCl, the Potentiometric Slope, and the Standard Deviation (SD) of the Standard Potential (E°) of the K-SCISEs^a

E_{prepol} (V) ^b	substrate	n^c	potential drift ($\mu\text{V h}^{-1}$) ^d	potential reproducibility, SD (mV)		slope (mV pK^{-1}) ^f	E° (SD; mV)
				$t = 0$ h	$t = 24$ h		
none	GC	5	-1100 ± 200	5.2	10.7	58.2 ± 0.7	10.9
0.22	GC	5	-56 ± 24^g	7.5 ^g	5.9 ^g	59.8 ± 0.2	5.9
0.4	GC	5	950 ± 130	3.3	2.7	58.1 ± 0.6	3.0
conventional K-ISE		5	32 ± 47^e	2.1	2.9	57.8 ± 0.5	3.0
0.22	Au	4	130 ± 210	4.0	6.4	N/A ^h	N/A
0.4	Au	4	-660 ± 330	7.1	7.8	N/A	N/A

^aWe show the conventional liquid contact K-ISE for comparison. ^bPrepolarization potential of the PEDOTF-SC vs a Ag wire in 0.01 M KTFAB-ACN. ^cNumber of electrodes. ^dDetermined between $t = 0.15$ and 24 h. ^eDetermined between $t = 0.10$ and 24 h. ^fDetermined in the concentration range of 10^{-5} – 10^{-1} M KCl. ^g $n = 4$. ^hNot measured due to the worse potential reproducibility in comparison to that for the K-SCISEs prepared on GC substrates.

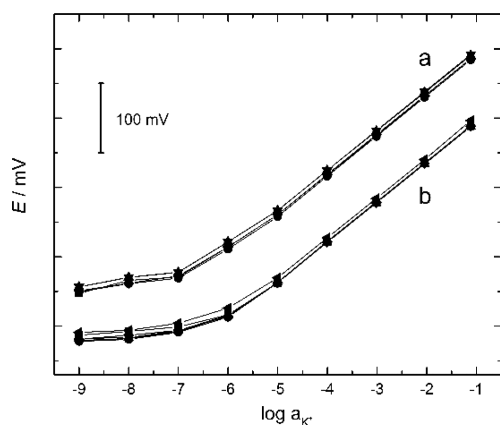


Figure 7. Potentiometric responses of (a) the K-SCISEs prepared on GC with the PEDOTF-SC prepolarized to 0.40 V ($n = 5$; vs a Ag wire) and (b) the conventional K-ISEs ($n = 5$) measured in 10^{-9} – 10^{-1} M KCl. The y axis scales are different for (a) and (b).

K-ISEs were ± 3.0 mV, 58.1 ± 0.6 mV pK^{-1} , and ca. 3×10^{-7} M and ± 3.0 mV, 57.8 ± 0.5 mV pK^{-1} , and ca. 5×10^{-7} M, respectively ($n = 5$). The same E° reproducibility indicates that inhomogeneities in the PVC-ISM may be the reason for or contribute significantly to the potential irreproducibility of the K-SCISEs. This may partially explain the differences in the E° reproducibilities reported in the literature. For example, Ishige et al. have recently reported a E° reproducibility of ± 0.6 mV ($n = 4$) for conventional plasticized PVC-based Li^+ -selective ISEs.²¹

The K-SCISEs prepolarized to the half-conducting form had a very low average potential drift of ca. $50 \mu\text{V h}^{-1}$ during 49 days, a potentiometric slope of 60.5 ± 0.1 mV pK^{-1} ($n = 4$), unchanged LOD (1×10^{-7} M), and E° reproducibility (± 5.5 mV) at the end of the test period. This shows that the PVC-ISM composition containing KTFAB, which was used for the first time in this work, is suitable for long-term use. The logarithmic selectivity coefficients of the K-SCISEs for the most relevant interfering ions were between -4.2 and -6.7 (except NH_4^+ ; Table S-1), which is in good accordance with other K-SCISEs with a similar PVC-ISM composition.⁹ The potentiometric aqueous layer test showed no water layer formation (Figure 8), and the chronopotentiometric measurements (Figure S-11) revealed that the SCISEs had a very low

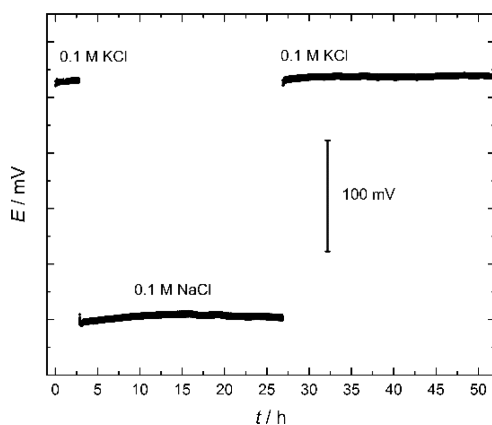


Figure 8. Potentiometric aqueous layer test performed with the K-SCISEs ($n = 3$) prepared on GC with the PEDOTF-SCs prepolarized to 0.22 V (vs a Ag wire).

potential change of only 1.2 ± 0.3 mV upon current polarization with ± 1 nA and no observable potential change when the current was decreased to ± 100 pA. The result of the aqueous layer test is in good accordance with the very low water uptake of the fluorinated PEDOTF-SC measured with the very sensitive FTIR-ATR technique. The chronopotentiometric measurements reveal that the redox capacitance of the buried SC was 2.2 ± 0.6 mF cm^{-1} , which is ca. 5% of the corresponding value of the bare PEDOTF-SC. However, this redox capacitance in combination with high hydrophobicity of the SC and the thermodynamically reversible charge (ion) transfer at the SC/ISM interface is sufficiently high to provide the K-SCISEs with a reproducible and stable potential.

CONCLUSIONS

We have fabricated K-SCISEs with the same E° reproducibility of ± 3.0 mV ($n = 5$) as that for the conventional liquid contact K-ISEs by using prepolarized and highly hydrophobic perfluorinated alkanolate side chain functionalized PEDOTF-TFAB as the SC (WCA: 133°). The SC had an outstanding potential reproducibility of ± 0.5 mV ($n = 6$) before the PVC-ISM was drop-cast on top of it. This indicates that the ISM deposition or inhomogeneities in the ISM is the main reason for the potential irreproducibility of the K-SCISEs. We believe this may have implications also for SCISEs with non-ECP solid contacts. We have fabricated altogether ca. 30 series of K-SCISEs and PEDOT-SCs, each consisting of four to six electrodes, and we believe therefore that ± 3.0 mV is the highest E° reproducibility that can be achieved with a higher number of K-SCISEs. They showed excellent response characteristics with conditioning times ≤ 5 min, low potential drift of ca. $50 \mu\text{V h}^{-1}$ over 49 days, almost ideal Nernstian slopes, no O_2 and CO_2 sensitivity, and no water layer formation. In addition, the bare PEDOTF-SC had no light sensitivity.

ASSOCIATED CONTENT

Supporting Information

The Supporting Information is available free of charge on the ACS Publications website at DOI: 10.1021/acs.analchem.9b01587.

EDOTF synthesis, GC substrates (CV characterization), PEDOTF-SC (SEM images, water uptake (experimental description), electropolymerization (CV, constant potential), impedance spectra) SCISEs (O_2 and CO_2 sensitivity (experimental description), initial potential stability, and reproducibility (Au substrates), calibration graphs, chronopotentiograms, impedance spectra, and selectivity coefficients) (PDF)

AUTHOR INFORMATION

Corresponding Author

*E-mail for T.L.: Tom.Lindfors@abo.fi.

ORCID

Márton Bojtár: 0000-0001-8459-4659

Róbert E. Gyurcsányi: 0000-0002-9929-7865

Tom Lindfors: 0000-0002-7119-5031

Author Contributions

M.B. synthesized EDOTF. S.P. carried out the experimental work except for Figure 1 and Figures S-2 and S-6. T.L. planned the work with S.P. and R.E.G. and wrote the first manuscript

draft. All authors have given their approval to the final version of the manuscript.

Notes

The authors declare no competing financial interest.

ACKNOWLEDGMENTS

T.L. gratefully acknowledges Dr. Hsiao-hua (Bruce) Yu at the RIKEN Advanced Science Institute (Japan) for the small amount of EDOTF that we received in January 2013 for preliminary experiments. Dr. Lajos Höfler is gratefully acknowledged for the mathematical modeling of the water diffusion in PEDOTF-SC. S.P. thanks the Johan Gadolin Process Chemistry Centre for the 3 month scholarship to Åbo Akademi University. T.L. gratefully acknowledges the Magnus Ehrnrooth Foundation for the travel grant to Budapest University of Technology and Economics in May–June 2018. The work was supported by the BME-Nanotechnology FIKP grant of EMMI (BME FIKP-NAT).

REFERENCES

- (1) Lindner, E.; Gyurcsányi, R. E. *J. Solid State Electrochem.* **2009**, *13*, 51–68.
- (2) Oyama, N.; Hirokawa, T.; Yamaguchi, S.; Ushizawa, N.; Shimomura, T. *Anal. Chem.* **1987**, *59*, 258–262.
- (3) Cadogan, A.; Gao, Z.; Lewenstam, A.; Ivaska, A.; Diamond, D. *Anal. Chem.* **1992**, *64*, 2496–2501.
- (4) Bobacka, J. *Anal. Chem.* **1999**, *71*, 4932–4937.
- (5) Lindfors, T.; Ivaska, A. *Anal. Chem.* **2004**, *76*, 4387–4394.
- (6) Lindfors, T.; Aarnio, H.; Ivaska, A. *Anal. Chem.* **2007**, *79*, 8571–8577.
- (7) Gyurcsányi, R. E.; Nybäck, A. S.; Tóth, K.; Nagy, G.; Ivaska, A. *Analyst* **1998**, *123*, 1339–1344.
- (8) He, N.; Gyurcsányi, R. E.; Lindfors, T. *Analyst* **2016**, *141*, 2990–2997.
- (9) He, N.; Papp, S.; Lindfors, T.; Höfler, L.; Latonen, R. M.; Gyurcsányi, R. E. *Anal. Chem.* **2017**, *89*, 2598–2605.
- (10) Guzinski, M.; Jarvis, J. M.; D’Orazio, P.; Izadyar, A.; Pendley, B. D.; Lindner, E. *Anal. Chem.* **2017**, *89*, 8468–8475.
- (11) Lai, C. Z.; Fierke, M. A.; Stein, A.; Bühlmann, P. *Anal. Chem.* **2007**, *79*, 4621–4626.
- (12) Crespo, G. A.; Macho, S.; Rius, F. X. *Anal. Chem.* **2008**, *80*, 1316–1322.
- (13) Fierke, M. A.; Lai, C. Z.; Bühlmann, P.; Stein, A. *Anal. Chem.* **2010**, *82*, 680–688.
- (14) Hernandez, R.; Riu, J.; Bobacka, J.; Valles, C.; Jimenez, P.; Benito, A. M.; Maser, W. K.; Rius, F. X. *J. Phys. Chem. C* **2012**, *116*, 22570–22578.
- (15) Hu, J.; Zou, X. U.; Stein, A.; Bühlmann, P. *Anal. Chem.* **2014**, *86*, 7111–7118.
- (16) Zou, X. U.; Cheong, J. H.; Taitt, B. J.; Bühlmann, P. *Anal. Chem.* **2013**, *85*, 9350–9355.
- (17) Zou, X. U.; Zhen, X. V.; Cheong, J. H.; Bühlmann, P. *Anal. Chem.* **2014**, *86*, 8687–8692.
- (18) Zhen, X. V.; Rousseau, C. R.; Bühlmann, P. *Anal. Chem.* **2018**, *90*, 11000–11007.
- (19) Piek, M.; Piech, R.; Paczosa-Bator, B. *J. Electrochem. Soc.* **2015**, *162*, B257–B263.
- (20) Paczosa-Bator, B.; Piek, M.; Piech, R. *Anal. Chem.* **2015**, *87*, 1718–1725.
- (21) Ishige, Y.; Klink, S.; Schuhmann, W. *Angew. Chem., Int. Ed.* **2016**, *55*, 4831–4835.
- (22) Klink, S.; Ishige, Y.; Schuhmann, W. *ChemElectroChem* **2017**, *4*, 490–494.
- (23) Bartoszewicz, B.; Dabrowska, S.; Lewenstam, A.; Migdalski, J. *Sens. Actuators, B* **2018**, *274*, 268–273.
- (24) Li, J. H.; Yin, T. J.; Qin, W. *Anal. Chim. Acta* **2015**, *876*, 49–54.
- (25) Ye, J. J.; Li, F. H.; Gan, S. Y.; Jiang, Y. Y.; An, Q. B.; Zhang, Q. X.; Niu, L. *Electrochem. Commun.* **2015**, *50*, 60–63.
- (26) Matzeu, G.; Zuliani, C.; Diamond, D. *Electrochim. Acta* **2015**, *159*, 158–165.
- (27) Yin, T. J.; Pan, D. W.; Qin, W. *Anal. Chem.* **2014**, *86*, 11038–11044.
- (28) Zeng, X. Z.; Yu, S. Y.; Yuan, Q.; Qin, W. *Sens. Actuators, B* **2016**, *234*, 80–83.
- (29) Mendecki, L.; Mirica, K. A. *ACS Appl. Mater. Interfaces* **2018**, *10*, 19248–19257.
- (30) Piek, M.; Piech, R.; Paczosa-Bator, B. *J. Electrochem. Soc.* **2016**, *163*, B573–B579.
- (31) Piek, M.; Piech, R.; Paczosa-Bator, B. *Electrochim. Acta* **2016**, *210*, 407–414.
- (32) Boeva, Z. A.; Lindfors, T. *Sens. Actuators, B* **2016**, *224*, 624–631.
- (33) Paczosa-Bator, B. *Carbon* **2015**, *95*, 879–887.
- (34) Sun, Q.; Li, W.; Su, B. *J. Electroanal. Chem.* **2015**, *740*, 21–27.
- (35) Jaworska, E.; Naitana, M. L.; Stelmach, E.; Pomarico, G.; Wojciechowski, M.; Bulska, E.; Maksymiuk, K.; Paolesse, R.; Michalska, A. *Anal. Chem.* **2017**, *89*, 7107–7114.
- (36) Li, J. H.; Yin, T. J.; Qin, W. *Sens. Actuators, B* **2017**, *239*, 438–446.
- (37) Liang, R.; Yin, T.; Qin, W. *Anal. Chim. Acta* **2015**, *853*, 291–296.
- (38) Bandodkar, A. J.; Molinnus, D.; Mirza, O.; Guinovart, T.; Windmiller, J. R.; Valdes-Ramirez, G.; Andrade, F. J.; Schoning, M. J.; Wang, J. *Biosens. Bioelectron.* **2014**, *54*, 603–609.
- (39) Gao, W.; Emaminejad, S.; Nyein, H. Y. Y.; Challa, S.; Chen, K. V.; Peck, A.; Fahad, H. M.; Ota, H.; Shiraki, H.; Kiriya, D.; Lien, D. H.; Brooks, G. A.; Davis, R. W.; Javey, A. *Nature* **2016**, *529*, 509–514.
- (40) Vanamo, U.; Bobacka, J. *Anal. Chem.* **2014**, *86*, 10540–10545.
- (41) Lindfors, T. *J. Solid State Electrochem.* **2009**, *13*, 77–89.
- (42) He, N.; Höfler, L.; Latonen, R.-M.; Lindfors, T. *Sens. Actuators, B* **2015**, *207*, 918–925.
- (43) Vanamo, U.; Bobacka, J. *Electrochim. Acta* **2014**, *122*, 316–321.
- (44) Schwendeman, I.; Gaupp, C. L.; Hancock, J. M.; Groenendaal, L.; Reynolds, J. R. *Adv. Funct. Mater.* **2003**, *13*, 541–547.
- (45) Luo, S. C.; Sekine, J.; Zhu, B.; Zhao, H. C.; Nakao, A.; Yu, H. H. *ACS Nano* **2012**, *6*, 3018–3026.
- (46) Lindfors, T.; Sundfors, F.; Höfler, L.; Gyurcsányi, R. E. *Electroanalysis* **2009**, *21*, 1914–1922.
- (47) Chen, P. H.; McCreery, R. L. *Anal. Chem.* **1996**, *68*, 3958–3965.
- (48) Nioradze, N.; Chen, R.; Kurapati, N.; Khyataeva-Domanov, A.; Mabic, S.; Amemiya, S. *Anal. Chem.* **2015**, *87*, 4836–4843.
- (49) Robinson, L.; Isaksson, J.; Robinson, N. D.; Berggren, M. *Surf. Sci.* **2006**, *600*, L148–L152.
- (50) Sundfors, F.; Lindfors, T.; Höfler, L.; Gyurcsányi, R. E. *Anal. Chem.* **2009**, *81*, 5925–5934.
- (51) Lindfors, T.; Höfler, L.; Jággerszki, G.; Gyurcsányi, R. E. *Anal. Chem.* **2011**, *83*, 4902–4908.
- (52) He, N.; Lindfors, T. *Anal. Chem.* **2013**, *85*, 1006–1012.
- (53) Fibbioli, M.; Morf, W. E.; Badertscher, M.; de Rooij, N. F.; Pretsch, E. *Electroanalysis* **2000**, *12*, 1286–1292.
- (54) Österholm, A.; Lindfors, T.; Kauppila, J.; Damlin, P.; Kvarnström, C. *Electrochim. Acta* **2012**, *83*, 463–470.
- (55) Lindfors, T.; Latonen, R.-M. *Carbon* **2014**, *69*, 122–131.